ATMOSPHERIC CORRECTION OF IMAGING SPECTROSCOPY DATA USING SHADOW-BASED QUANTIFICATION OF AEROSOL SCATTERING EFFECTS

Daniel Schläpfer[1], and Rudolf Richter[2]

1. ReSe Applications, Wil SG, Switzerland; daniel(at)rese.ch
2. German Aerospace Center (DLR), Wessling, Germany; rudolf.richter(at)dlr.de

ABSTRACT

The atmospheric correction accuracy strongly depends on the correct estimate of the aerosol scattering effects. This paper shows first results of a new aerosol optical thickness inversion method and its use for improved atmospheric correction of high spatial resolution imaging spectroscopy data. The approach uses small scale shadow pixels for the determination of the atmospheric scattering by inverting the shadow correction within the ATCOR® atmospheric compensation method. The detection of shadow pixels is done by a blue to red ratio which is further adjusted by the near infrared band in order to take the vegetation bias into account. On high resolution instruments with resolutions below 5 m, a decent quantity of shaded pixels can be found by this method in a reliable way. Using this shadow mask, the aerosol inversion is done. The aerosol contents are varied in a way that retrieves a correction of shaded areas to a brightness comparable to non-shaded areas, leading to the best fitting aerosol amount. The shadow based aerosol optical thickness (SHAOT) method is tested on APEX and HYSPEX airborne imaging spectroscopy data. It can be shown that the atmospheric compensation using the such derived aerosol contents are significantly improved in comparison to standard correction techniques.

KEYWORDS

Atmospheric correction, radiometric compensation, haze and dust correction, atmospheric scattering, SHAOT, ATCOR.

INTRODUCTION

Atmospheric correction methods have been developed for many years now and are standard procedures for optical satellite and airborne data preprocessing (1). The methods have evolved from simple correction of virtually uncalibrated at-sensor digital numbers by empirical methods to physical atmospheric compensation of atmospheric effects from calibrated at-sensor radiances using radiative transfer code simulations. The aerosol optical thickness (*AOT*) is a key parameter for such atmospheric compensation techniques. The retrieval and correction of *AOT* from airborne optical remote sensing and spectroscopy data is a task which has been investigated for many years. A prominent method currently used to compensate for aerosol effects in optical remote sensing data is the dense dark vegetation approach (DDV, (2)). It relies on the presence of vegetated areas and uses an empirically found correlation between the visible and near or short-wave infrared reflectance to find the signatures of aerosols in the visible bands. This method is limited to data containing dark vegetation such as forests. Therefore, further methods have been investigated which either make use of optimisation schemes with simultaneous aerosol and reflectance retrievals (3,4), or rely on multi-sensor integration (5). Iterative adaption of aerosol parameters has been applied for cloud shadow correction from imaging spectroscopy data over water in earlier studies by comparing the shaded areas to directly illuminated reference sections (6,7).

Another widely used approach for aerosol and haze detection and correction is the dark object analysis and subtraction method (DOS, (8,9)). It is specifically suited for dense aerosol layers and haze. Using a moving window technique, this method has been further developed for statistical

DOI: 10.12760/01-2017-1-03

haze detection and removal (10). However, the underlying reflectance signature does not allow for accurate aerosol optical thickness determination in relatively clear atmospheres.

Recent experience by the authors has shown limitations of the DDV method for high spatial resolution data (i.e., spatial resolutions between 0.1 and 5 m), where numerous small-scale shadows and dark objects are disturbing the process. No ready to use alternative aerosol detection routine is available for operational use on this kind of data. To further advance the aerosol optical thickness detection in support of atmospheric compensation of such data, a new approach is investigated in this paper. The authors have observed that compensation of shadows by radiometric de-shadowing in the ATCOR® method (11) shows a very high sensitivity of the de-shadowing process from the aerosol contents. This sensitivity can be used for aerosol content derivation. The inversion of the de-shadowing process may lead to the optimal aerosol content. Using shadows instead of dark vegetation bears the advantage that shaded pixels can be found in most high-resolution imagery. The method is not applicable if the data was recorded for very small solar zenith angles or over completely flat areas such as salt lakes or extended agricultural fields.

METHOD

A precondition to the analysis of shadow signatures is the knowledge about the location of shaded pixels. A shadow detection method is used, which exploits the difference of the spectral signatures of shaded pixels in comparison to the directly illuminated pixels to detect cast shadow areas. This shadow detection approach has been further developed from an idea presented in (12). The method uses a red-blue shadow index which is calculated as:

$$Ind_{rb} = \frac{\rho_r}{\rho_b - c_n\left[\left(\rho_n - \rho_r\right)\right]}$$

where ρ_r, ρ_b and ρ_n are the apparent reflectances in the red, blue and near infrared channels, respectively, and the correction of vegetation influence is only included for $\left(\rho_n - \rho_r\right) > 0$. The empirical correction factor c_n accounts for vegetation influences, it is typically set to a value of 0.08. Thresholds are set on the combined index to derive a shading map with transition between full cast shadow and illuminated areas (compare Figure 1). The method uses selected spectral channels closest to 450, 670, and 780 nm for blue, red and near infrared, respectively.

This cast shadow map is then used in conjunction with the ATCOR® atmospheric compensation approach (13) and the therein contained atmospheric look-up-table (LUT) for *AOT* determination. The LUTs are based on MODTRAN®5 (14), whereas the ATCOR model and the therein contained cast shadow removal routine is described in detail in (13). In an iterative procedure, the diffuse irradiance onto the cast shadow areas is tuned by varying the aerosol amount in the atmospheric compensation process until the corrected reflectance statistics in originally shaded areas are at the same brightness level as the adjacent areas with direct irradiance regime within a 0.05% difference in average reflectance. Using a moving window approach, *AOT* distribution maps can be derived by this technique at spectral bands in the visible wavelengths of the spectrum.

The complete retrieval procedure consists of the following steps:

1. prepare calibrated image, DEM, and ATCOR LUT for the observation geometry,
2. transform image to at-sensor reflectance,
3. run shadow detection routine to create cast shadow layer,
4. update sky view factor layer to account for reduced sky view in cast shadow areas,
5. start moving window on one selected image band (e.g., at 550 nm).
    a. create image subsets including DEM, shadow mask, sky view factor, and reduced atmospheric LUT for subset,
    b. find bright reference mask in vicinity of 20 pixels from cast shadow pixels (while excluding dark pixels).

   c. check if subset statistics are sufficient for iteration; skip if less than 100 shadow pixels are found.
   d. adjust aerosol content iteratively until the average reflectance in the corrected cast shadow areas match the bright reference areas, and
   e. store aerosol content for image patch.
6. write aerosol optical thickness distribution and visibility index for the whole image by triangulated bilinear interpolation and under consideration of the digital elevation model.

This shadow based aerosol optical thickness retrieval procedure (we name it "SHAOT") has been implemented in the ATCOR atmospheric and topographic compensation environment, making use of the terrain-dependent modelling of irradiance for each image pixel. The model takes into account the adjacency radiance as well as the local sky view factor which both are critical parameters for correct description of the diffuse irradiance on a pixel.

It has to be noted, that this method uses image statistics for its analysis. A minimum of 100 shaded pixels and 300 reference pixels per image patch have been set as limit to make the retrieval work with enough statistical viability.

RESULTS

In this paper, we focus on the application of this method to APEX (15) and Hyspex (16) imaging spectroscopy imagery, whereas first successful tests had been done on Leica ADS high resolution photogrammetric data.

Application to APEX data

The investigated sample data was acquired on June 29th 2010 over the Laegern site, Switzerland. The data was recorded at a flight altitude of 4.47 km a.s.l., the average ground altitude was at 0.53 km, the solar zenith was 29.3°, and the swath width was 4 km (across track).

An example of the shadow detection routine output is given in Figure 1. Most small-scale shadows are well detected in the imagery. The shown image subset is of the typical size of the image patches used as moving window for aerosol determination, at typical diameters of 500 - 1000 m.

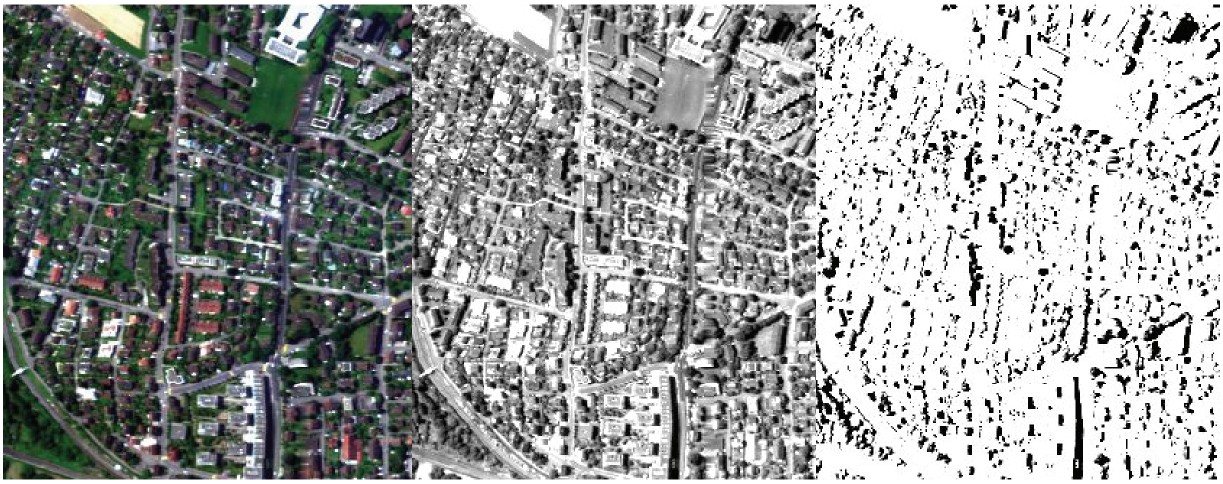

Figure 1: Cast shadow detection for APEX imagery; left: RGB image, middle: shadow index, right: cast shadow map after thresholding (index transition range 0.4 - 0.5).

An exemplary result for one of the images is shown in Figure 2. ATCOR atmospheric correction was implemented under consideration of topographic effects and using empirical incidence *BRDF* correction. Using the aerosol distribution earlier derived from the use of the DDV method led to undercorrections in the forested areas. The input of the SHAOT results for atmospheric compensation leads to a visible improvement. Image areas without dark vegetation or lacking shadow pixels, respectively, are interpolated by triangulation for both methods. The derived aerosol distribution maps from SHAOT show reasonable *AOT* values with increased amounts over the hilly forests, where convective streams may have led to an aerosol accumulation.

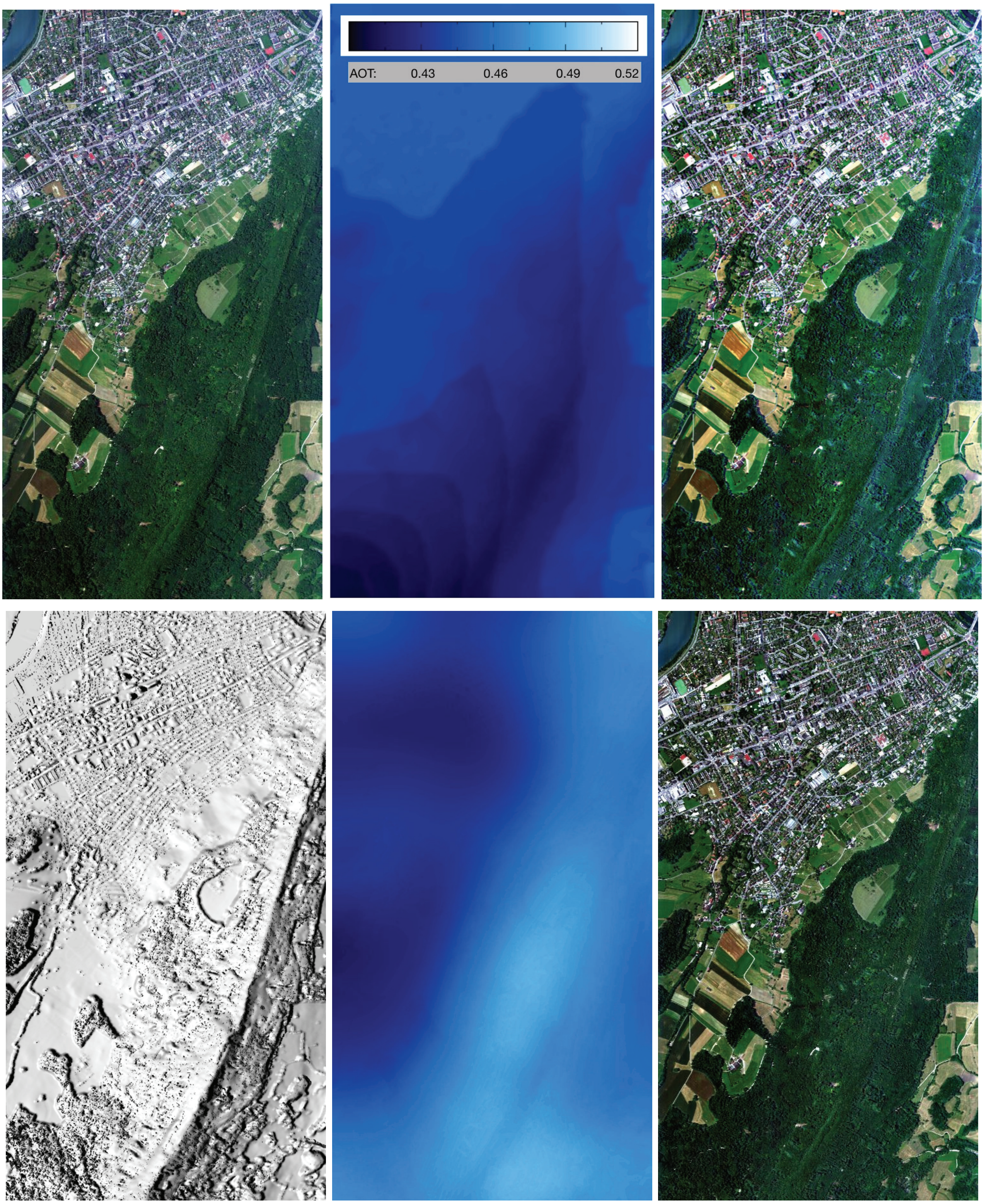

Figure 2: Example of aerosol retrieval and atmospheric compensation for APEX Laegern site: Top row: original image, DDV based aerosol retrieval and atmospheric compensation result. Bottom row: cast shadow map, SHAOT based aerosol retrieval and atmospheric compensation result.

If sample spectra are compared as shown in Figure 3, the difference between the standard aerosol correction and the SHAOT result is clearly visible. In the blue spectral range, the higher aerosol amounts found from shadow analysis lead to lower reflectance values for dark vegetation which is a more realistic spectrum for such objects. For a bright asphalt object, no such difference is visible in the blue since aerosol scattering and absorption cancel each other out at high reflectance levels. However, a clear difference is visible in the near infrared, where the adjacency effects from the dominant vegetation areas are insufficiently corrected with the lower aerosol amounts, whereas the reflectance level is appropriate using the SHAOT aerosol amount. It has to be noted, that the spectra have not been smoothed or polished in these graphs, which results in visible spectral spikes in the data.

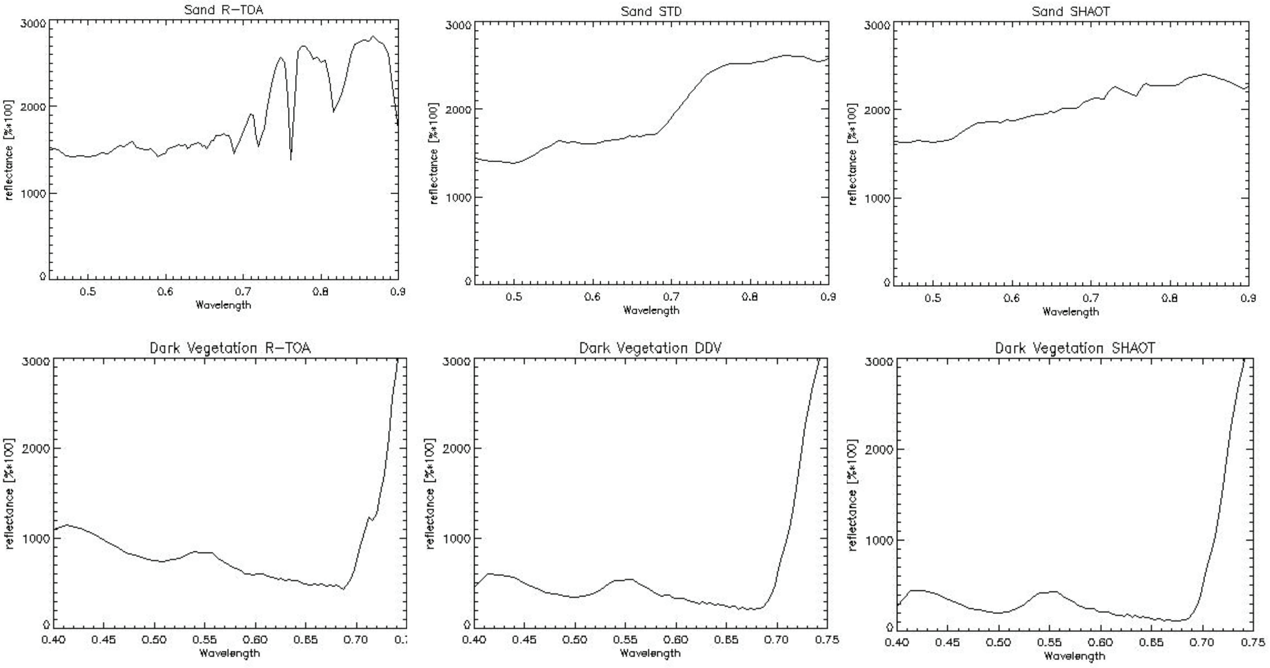

Figure 3: Spectral impact of aerosol content estimation on atmospheric compensation results. Left: at-sensor reflectance spectra, middle: atmospheric compensation with standard aerosol contents, right: atmospheric compensation with SHAOT based aerosol contents; wavelengths given in nm.

Application to Hyspex-Data

A second sample data set was acquired Sept. 19th 2016 by the HySpex VNIR 1600 instrument in French Guyana by CNES France, mapping rain forest areas. For this data acquisition, the solar zenith angle was between 22° and 24° at a flight altitude of 700 - 800 m above ground and a swath width of 250 m. The rain forest imagery was affected by faint mist due to the humid environment which results in highly variable atmospheric conditions. An accurate aerosol correction is required for improving the consistency of the ground spectra for tree species mapping. The results of the process for two overlapping image strips are shown in

Figure 4. The aerosol variations cannot be corrected by standard atmospheric compensation, and also DDV based processing did not show any advantage (not shown in the Figure). Using the SHAOT approach, a reasonable *AOT* map can be derived which significantly improves the atmospheric correction result. As observer *BRDF* effects are not covered by the atmospheric compensation, a final BREFCOR processing (17) further improves the resulting reflectance homogeneity within and between the two mage strips.

Three spectral average samples of 200 × 200 pixels in the overlap area are shown in Figure 5. The SHAOT method significantly reduces the difference between the two data acquisitions. Remaining offsets are due to the variations in self shadowing between the two data acquisitions.

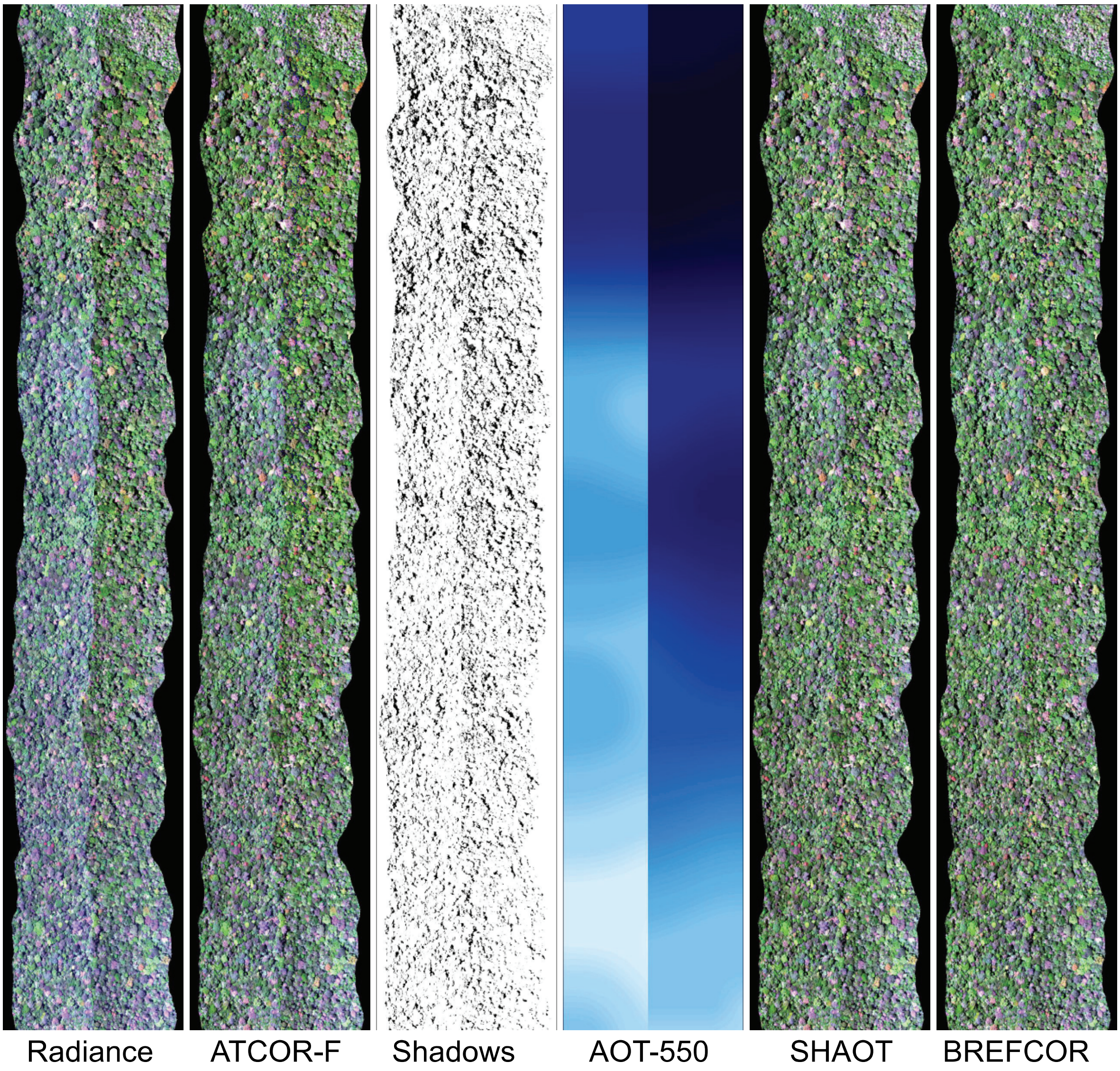

Figure 4: Processing of Hyspex imagery in a tropical environment: left radiance imagery and reflectance after standard atmospheric compensation with fixed aerosol amount. Middle: shadow detection and derived AOT at 550 nm, scale ranging from 0.20 to 0.34. Right: atmospheric compensation using the SHAOT-based AOT distribution and final processing with the BREFCOR method.

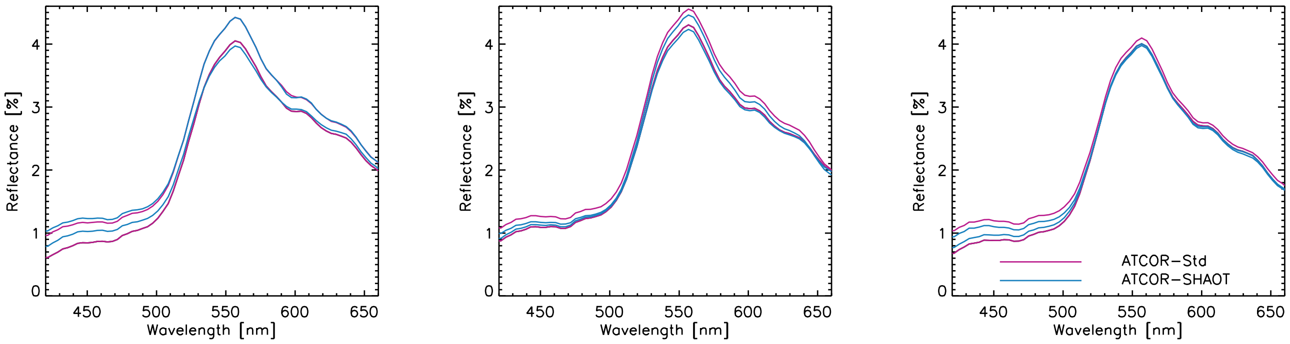

Figure 5: Impact of SHAOT based atmospheric compensation on spectra in the visible range in overlap regions. The three graphs show averaged spectra of three samples.(200 × 200 pixels) in the overlapping area for the original ATCOR processing using DDV derived aerosol amounts and the ATCOR processing using the SHAOT derived aerosol amounts.

CONCLUSIONS

An alternative retrieval method for aerosol optical thickness in support of atmospheric compensation has been shown. It uses an inversion of the ATCOR routine to define the aerosol contents over shaded areas. The method is well applicable for high resolution imagery at resolutions below 5 m, as long as enough pixels in cast shadows are available. As the method is using a moving window technique, the statistics in the moving window over hundreds of pixels are used for the inversion – single pixel inversion is not feasible as the local irradiance regime cannot be modelled to this level of accuracy by the current implementation of ATCOR.

The method is limited by the availability of spatially distributed cast shadow areas and therefore, it only works successfully on high resolution images. A further limitation is the instrument dynamics. The dark cast shadows should namely still be registered with enough fidelity to distinguish surface characteristics. Furthermore, results will be hard to retrieve for high ground altitude data and very clear atmospheres as the diffuse irradiance is very low for such situations.

The method will be further developed toward full operationality for both, high resolution satellite and airborne imagery. Furthermore, it bears the potential to derive the *AOT* values throughout the visible part of the spectrum by inverting the aerosol amount at various wavelengths. Based on a such extended retrieval, the method could theoretically be used to characterise the spectral aerosol by single scattering albedo and aerosol size distribution from imagery.

Another potential application of this method is the pixel-wise cast shadow correction. So far, only average correction factors can be found from the method, which leads to strong variation of correction results and related image artifacts within corrected cast shadow areas. New methods have to be found to include more information about the irradiance from adjacent objects to a pixel and to include statistical neighbourhood analysis in order to achieve seamless cast shadow correction.

ACKNOWLEDGEMENTS

The Remote Sensing Laboratories of the University of Zürich are acknowledged for providing the APEX data. CNES France and Marc Lennon from Hytech-Imaging are gratefully acknowledged for providing the Hyspex data.

REFERENCES

1 Gao B-C, M J Montes, C O Davis & A F H Goetz, 2009. Atmospheric correction algorithms for hyperspectral remote sensing data of land and ocean, Remote Sensing of Environment, 113(1): S17-S24

2 Kaufman Y J & C Sendra, 1988. Algorithm for automatic atmospheric corrections to visible and near-IR satellite imagery, International Journal of Remote Sensing, 9(8): 1357-1381

3 Guanter L, L Gomez-Chova & J Moreno, 2008. Coupled retrieval of aerosol optical thickness, columnar water vapor and surface reflectance maps from ENVISAT/MERIS data over land, Remote Sensing of Environment, 112(6): 2898-2913

4 Govaerts Y & M Luffarelli, 2017. Joint retrieval of surface reflectance and aerosol properties with continuous variations of the state variables in the solution space: Part 1: theoretical concept. Atmospheric Measurements Techniques, Discussion papers

5 Dubovik O, T Lapyonok, P Litvinov, M Herman, D Fuertes, F Ducos, B Torres, Y Derimian, X Huang, A Lopatin, A Chaikovsky, M Aspetsberger & C Federspiel, 2014. GRASP: a versatile algorithm for characterizing the atmosphere. SPIE Newsroom,
DOI: 10.1117/2.1201408.005558

6 Reinersman P, K L Carder & F R Chen, 1998. Satellite-sensor calibration verification with the cloud-shadow method. Applied Optics, 37: 5541-5549

7 Amin R, D Lewis, R Gould, W Hou, A Lawson, M Ondrusek & R Arnone, 2014. Assessing the application of cloud shadow atmospheric correction algorithm on HICO. IEEE Transactions on Geoscience Remote Sensing, 52(5): 2646-2653

8 Chavez P S Jr., 1988. An improved dark-object subtraction technique for atmospheric scattering correction of multispectral data. Remote Sensing of Environment, 24(3): 459-479

9 Gonima L, 1993. Simple Algorithm for the Atmospheric Correction of Reflectance Images. International Journal of Remote Sensing, 14: 1179-1187

10 Makarau A, R Richter, D Schläpfer & P Reinartz, 2016. Combined haze and cirrus removal for multispectral imagery, IEEE Geoscience and Remote Sensing Letters, 13(3): 379-383

11 Richter R & D Schläpfer, 2002. Geo-atmospheric processing of airborne imaging spectrometry data. Part 2: Atmospheric/Topographic Correction. International Journal of Remote Sensing, 23(13): 2631-2649

12 Schläpfer D, R Richter & A Damm, 2013. Correction of shadowing In imaging spectroscopy data by quantification of the proportion of diffuse illumination. Presented at the 8th SIG-IS EARSeL Imaging Spectroscopy Workshop, Nantes, 8-13 April 2013 (last date accessed: 15 Nov 2017)

13 Richter R & D. Schläpfer, 2017. Atmospheric / Topographic Correction for Satellite Imagery, ATCOR-4 User Guide, Version 7.1.2. DLR/ReSe, Wessling, DLR-IB 565-02/17, Oct 2017

14 Berk A, G P Anderson, P K Acharya, L S Bernstein, L Muratov, J Lee, M J Fox, S M Adler-Golden, J H Chetwynd, M L Hoke, R B Lockwood, J A Gardner, T W Cooley & P E Lewis, 2004. MODTRAN5: a reformulated atmospheric band model with auxiliary species and practical multiple scattering options. Proc. SPIE: 5571, Remote Sensing of Clouds and the Atmosphere IX (30 November 2004); doi: 10.1117/12.564634

15 Schaepman M E, M Jehle, A Hueni, P D'Odorico, J Weyermann, F D Schneider, V Laurent, C Popp, F C Seidel, K Lenhard, P Gege, C Küchler, J Brazile, ,P Kohler, L De Vos, K Meuleman, R Meynart, D Schläpfer, M Kneubühler & K I Itten, 2015. Advanced radiometry measurements and Earth science applications with the Airborne Prism Experiment (APEX), Remote Sensing of Environment, 158: 207-219

16 Köhler C H, 2014: Airborne Imaging Spectrometer HySpex. Journal of Large-Scale Facilities JLSRF, 2, A93, 6 pp.

17 Schläpfer D, R Richter & T Feingersh, 2015. Operational BRDF effects correction for wide-field-of-view optical scanners (BREFCOR). IEEE Transactions on Geoscience and Remote Sensing, 53(4): 1855-1864